Black hole binary formation in the expanding universe: Three body problem approximation

Kunihito Ioka,[1] Takeshi Chiba,[2] Takahiro Tanaka,[3] and Takashi Nakamura[4]
[1]*Department of Physics, Kyoto University, Kyoto 606-01, Japan*
[2]*Department of Physics, University of Tokyo, Tokyo 113-0033, Japan*
[3]*Department of Earth and Space Science, Osaka University, Toyonaka 560, Japan*
[4]*Yukawa Institute for Theoretical Physics, Kyoto University, Kyoto 606-01, Japan*
(Received 9 February 1998; published 27 August 1998)

We study black hole MACHO binary formation through three-body interactions in the early universe at $t \sim 10^{-5}$ s. The probability distribution functions of the eccentricity and the semimajor axis of binaries as well as of the coalescence time are obtained assuming that the black holes are randomly formed in space. We confirm that the previous order-of-magnitude estimate for the binary parameters is valid within $\sim 50\%$ error. We find that the coalescence rate of the black hole MACHO binaries is $\sim 5 \times 10^{-2} \times 2^{\pm 1}$ events/yr/galaxy, taking into consideration several possible factors which may affect this estimate. This suggests that the event rate of coalescing binary black holes will be at least several events per year within 15 Mpc. The first LIGO-VIRGO interferometers in 2001 will be able to verify whether or not the MACHOs are black holes. [S0556-2821(98)06018-4]

PACS number(s): 97.60.Lf, 04.30.−w, 95.35.+d, 98.80.Bp

I. INTRODUCTION

The analysis of the first 2.1 years of photometry of 8.5×10^6 stars in the Large Magellanic Cloud (LMC) by the MACHO Collaboration [1] suggests that the fraction $0.62^{+0.3}_{-0.2}$ of the halo consists of MACHOs (massive compact halo objects) of mass $0.5^{+0.3}_{-0.2} M_\odot$ in the standard spherical flat rotation halo model. The preliminary analysis of four years of data suggests the existence of at least four additional microlensing events with $t_{dur} \sim 90$ days in the direction of the LMC [2]. At present, we do not know what MACHOs are. This is especially because there are strong degeneracies in any microlensing measurements: the mass, velocity and distance of a lens object. The inferred mass is just the mass of red dwarfs. However, a tight constraint is obtained from the observations [3–5]. The red dwarfs contribute at most a few percent to the mass of the halo.

The brown dwarfs are also restricted by the *Hubble Space Telescope* search. Extrapolating the mass function, the contribution of the brown dwarfs to the mass of the halo is less than a few percent [5]. However, the possibility of brown dwarfs cannot be rejected if the mass function has a peak at the brown dwarfs since they are so dim. The possibility that the MACHOs are neutron stars is ruled out by the observational constraints on the metal and helium abundance [6].

As for white dwarfs, assuming the Salpeter initial mass function (IMF) with an upper and a lower mass cutoff, the mass fraction of the white dwarfs in the halo should be less than 10% from the number count of the high z galaxies [7]. The observation of the chemical yield does not favor the MACHOs being white dwarfs [8,9]. However, if the IMF has a peak around $\sim 2 M_\odot$, MACHOs can be white dwarfs [10–12]. Future observations of high-velocity white dwarfs in our solar neighborhood will make clear whether or not white dwarf MACHOs exist. Of course, it is still possible that an overdense clump of MACHOs exists toward the LMC [13].

If the number of high-velocity white dwarfs turns out to be large enough to explain the MACHOs, then star formation theory should explain why the IMF has a peak at $\sim 2 M_\odot$. If it is not, we must consider other possibilities such that MACHOs are primordial black holes or boson stars. If MACHOs are black holes, however, it seems difficult to verify observationally whether the MACHOs are black holes or not. In fact, electromagnetic radiation from gas accreting to a black hole MACHO (BHMACHO) is too dim to be observed unless the velocity of the BHMACHO is exceptionally small [14].

Recently, however, Nakamura *et al.* [15] proposed the detectability of the gravitational wave from coalescence of BHMACHO binaries which are formed through a three body interaction in the early universe at $t \sim 10^{-5}$ s. The event rate of coalescing BHMACHO binaries was estimated as $\sim 5 \times 10^{-2}$ events/yr/galaxy, which suggests that we can expect several events per year within 15 Mpc. If this estimate is true, not only can we confirm whether the MACHOs are black holes or not, but also we have plenty of sources of gravitational waves. However, in Ref. [15] they made only order-of-magnitude arguments and there are uncertainties in the estimate of the event rate. Especially, the estimate of the semimajor and semiminor axes of the binary formed through the three body interaction is not based on accurate numerical calculations. In this paper we investigate up to what extent the order-of-magnitude arguments in Ref. [15] are valid by calculating numerically the three body problem in an expanding universe.

In Sec. II we will review the formation scenario of the BHMACHO binaries in Ref. [15]. In Sec. III we will derive the basic equations of a multi-particle system in the expanding universe. In Sec. IV we will show the results of the numerical calculations of the binary formation through the three body interaction in the expanding universe. In Sec. V we will obtain the probability distribution functions of the eccentricity and the semimajor axis of binaries as well as the coalescence time assuming that the black holes are randomly formed in space. We will estimate the event rate of coalesc-

ing binaries using this probability distribution function. In Sec. VI we will consider several possible factors which may affect the estimate of the event rate, and we will conclude that the event rate is not reduced considerably. In Sec. VII we will consider how BHMACHO binaries evolve after the binary formation. Section VIII will be devoted to a summary and discussion.

We use units of $G=c=1$ in this paper.

II. REVIEW OF THE BHMACHO BINARY FORMATION SCENARIO

We briefly review the BHMACHO binary formation scenario in Ref. [15] to introduce our notations.

For simplicity, we assume that black holes dominate dark matter, i.e. $\Omega=\Omega_{BHM}$. The extension to the case where black holes do not dominate dark matter is not difficult. Further we assume that all black holes have the same mass and we describe it as M_{BH}. (The extension to the unequal mass case is straightforward and is given in the Appendix.) Primordial black holes are formed when the horizon scale is equal to the Schwarzschild radius of a black hole. There are some theories about the formation mechanism of primordial black holes [16–18]. At present, however, we cannot say definitely whether or not the black holes will form in the early universe. Ultimately, only by observational technique may the existence of a population of primordial black holes be established. It is therefore important to establish the observational signatures of primordial black holes. Our standpoint is that we are quite ignorant of whether or not large numbers of primordial black holes will form in the early universe, and it is very important to confirm the existence of primordial black holes observationally. Whether or not the results of the observation confirm the extistence of primordial black holes, it will add very much to our understanding of the universe.

The scale factor at the time of the formation is given by

$$R_f=\sqrt{M_{BH}/H_{eq}^{-1}}=1.1\times10^{-8}\left(\frac{M_{BH}}{M_\odot}\right)^{1/2}(\Omega h^2), \quad (2.1)$$

where H_{eq} with $H_{eq}^{-1}=\sqrt{3/8\pi\rho_{eq}}=1.2\times10^{21}(\Omega h^2)^{-2}$ cm is the Hubble parameter at the time of matter-radiation equality. We normalize the scale factor such that $R=1$ at the time of matter-radiation equality.

The mean separation of black holes $\bar{x}$ with mass M_{BH} at the time of matter-radiation equality is given by

$$\bar{x}=(M_{BH}/\rho_{eq})^{1/3}=1.2\times10^{16}(M_{BH}/M_\odot)^{1/3}(\Omega h^2)^{-4/3}\ \text{cm}. \quad (2.2)$$

As a foundation for computing the distribution function of BHMACHO binaries with respect to the binary parameters, in Ref. [15] it was assumed that (i) the BHMACHOs are created with a distribution of comoving separations x that is *uniform* over the range from an initial physical separation equal to the black hole size to a maximum separation $x=\bar{x}$ and that (ii) the BHMACHOs' initial peculiar velocity is negligible compared to the Hubble flow. Obviously, it is more realistic to assume that the BHMACHOs are formed *randomly* rather than uniformly. We will consider the effect of the initial peculiar velocity in Sec. VI D.

Consider a pair of black holes with the same mass M_{BH} and a comoving separation $x<\bar{x}$. These holes' masses produce a mean energy density over a sphere with the radius of the size of their separation as $\bar{\rho}_{BH}\equiv\rho_{eq}\bar{x}^3/(x^3R^3)$. $\bar{\rho}_{BH}$ becomes larger than the radiation energy density $\rho_r=\rho_{eq}/R^4$ if

$$R>R_m\equiv\left(\frac{x}{\bar{x}}\right)^3. \quad (2.3)$$

After $R=R_m$ the binary decouples from the cosmic expansion and becomes a bound system. The tidal force from neighboring black holes gives the binary sufficiently large angular momentum to keep the holes from colliding with each other unless x is exceptionally small.

The semimajor axis a will be proportional to xR_m. Hence, we have

$$a=\alpha xR_m=\alpha\frac{x^4}{\bar{x}^3}, \quad (2.4)$$

where α is a constant of order $O(1)$. To estimate the tidal torque, we assume that the tidal force is dominated by the black hole nearest to the binary. We denote by y the comoving separation of the nearest neighboring black hole from the center of mass of the binary. Then, from dimensional analysis, the semiminor axis b will be proportional to (tidal force)$\times$(free fall time)^2 and is given by

$$b=\alpha\beta\frac{M_{BH}xR_m}{(yR_m)^3}\frac{(xR_m)^3}{M_{BH}}=\beta\left(\frac{x}{y}\right)^3a, \quad (2.5)$$

where β is a constant of order $O(1)$. Hence, the binary's eccentricity e is given by

$$e=\sqrt{1-\beta^2\left(\frac{x}{y}\right)^6}. \quad (2.6)$$

In Ref. [15], $\alpha=\beta=1$ is assumed. However, α and β will be different from unity so that calculations of the distribution functions based on an accurate estimate of α and β are necessary. This is the prime subject of the present paper.

III. MULTI-PARTICLE SYSTEM IN THE EXPANDING UNIVERSE

Although our main interest is in the three body problem, we formulate the problem as generally as possible.

A. Basic equations

We treat the motion of a black hole as that of a test particle within the Newtonian approximation [19–21]. We first assume that the line element is given by

$$ds^2=-(1+2\phi)dt^2+(1-2\phi)R(t)^2d\mathbf{x}^2, \quad (3.1)$$

where ϕ is the Newtonian potential determined by

$$R^{-2}\Delta\phi = 4\pi\rho_{BH}, \tag{3.2}$$

with ρ_{BH} being the energy density of black holes. For the multi-particle system, the potential is readily solved as $\phi(\mathbf{x}) = -\Sigma_{\mathbf{j}} m_{\mathbf{j}}/R|\mathbf{x}-\mathbf{x}_{\mathbf{j}}|$, where $\mathbf{x}_{\mathbf{j}}$ is the position of the $\mathbf{j}$th black hole. The action of the particle is given by

$$\int ds = \int \sqrt{1+2\phi - R^2\dot{\mathbf{x}}^2}\,dt \simeq \int \left(1 - \frac{1}{2}R^2\dot{\mathbf{x}}^2 + \phi\right)dt. \tag{3.3}$$

Then the equation of motion is derived as

$$(R^2\dot{\mathbf{x}})^{\cdot} = -\nabla\phi. \tag{3.4}$$

For the potential, $\phi(\mathbf{x_i}) = -\Sigma_{\mathbf{j}\neq\mathbf{i}} m_{\mathbf{j}}/R|\mathbf{x_i}-\mathbf{x_j}|$, of the multi-particle system, the above equation is expressed as

$$(R^2\dot{\mathbf{x}}_{\mathbf{i}})^{\cdot} = -\frac{1}{R}\sum_{\mathbf{j}\neq\mathbf{i}} \frac{m_{\mathbf{j}}(\mathbf{x_i}-\mathbf{x_j})}{|\mathbf{x_i}-\mathbf{x_j}|^3}. \tag{3.5}$$

We introduce $\mathbf{z_i} \equiv \mathbf{x_i}/\overline{x}$ and use the scale factor R as an independent variable. Then for the equal-mass black hole case, Eq. (3.5) can be written as

$$\mathbf{z}_{\mathbf{i}}'' + \frac{1}{R}\mathbf{z}_{\mathbf{i}}' = -\frac{M_{BH}}{\overline{x}^3 H^2 R^5}\sum_{\mathbf{j}\neq\mathbf{i}} \frac{(\mathbf{z_i}-\mathbf{z_j})}{|\mathbf{z_i}-\mathbf{z_j}|^3} = -\frac{3}{8\pi R}\sum_{\mathbf{j}\neq\mathbf{i}} \frac{(\mathbf{z_i}-\mathbf{z_j})}{|\mathbf{z_i}-\mathbf{z_j}|^3}, \tag{3.6}$$

where a prime denotes the derivative with respect to R and we have used Eq. (2.2) in the last equality. Note that Eq. (3.6) does not depend on M_{BH}. Moreover, there is a scaling law: i.e., Eq. (3.6) is invariant under the transformation defined by

$$\mathbf{z} \to \lambda\mathbf{z}, \quad R \to \lambda^3 R, \tag{3.7}$$

where λ is a constant.

B. Validity of the Newtonian approximation

The cosmological Newtonian approximation is valid if (1) $|\phi| \ll 1$ and (2) the scale of inhomogeneity l satisfies the relation $l \ll H^{-1}$ [20,21]. Since the minimum separation between the binary black holes is $a(1-e)$, the condition (1) is satisfied if

$$M_{BH} \ll a(1-e). \tag{3.8}$$

Then in terms of the initial comoving separation we have

$$y/x \ll 5.8\times 10(x/\overline{x})^{2/3}(M_{BH}/M_{\odot})^{-1/9}(\Omega h^2)^{-2/9}, \tag{3.9}$$

where we used Eq. (2.4), Eq. (2.6) for $\alpha=\beta=1$ and the relation of $(1-e)\simeq(1-e^2)/2$. The condition (2) is written as

$$Rx \ll H_{eq}^{-1}R^2. \tag{3.10}$$

Then we have

$$R \gg 1.0\times 10^{-5}(x/\overline{x})(M_{BH}/M_{\odot})^{1/3}(\Omega h^2)^{2/3}. \tag{3.11}$$

Therefore we have to choose the initial scale factor for the numerical calculations so that the condition (3.11) is satisfied.

IV. THREE BODY PROBLEM AND FORMATION OF BINARY BLACK HOLES

We solve Eq. (3.6) numerically for three body systems using the fifth-order Runge-Kutta method with the adaptive step size control [22]. Considering the conditions for the validity of the Newtonian approximation derived in the previous section, we set the initial conditions as $x/\overline{x} = \eta (0.1 < \eta < 1)$ and $\dot{x} = 0$ at $R = 10^{-3}\eta(M_{BH}/0.5M_{\odot})^{1/3}$ so that Eq. (3.11) is satisfied, where we place a pair of black holes along the x-axis. Note that, using the scaling law of Eq. (3.7), we see that these initial conditions are the same as $x/\overline{x} = \lambda\eta$ and $\dot{x} = 0$ at $R = 10^{-3}(\lambda\eta)(M_{BH}/0.5\lambda^{-6}M_{\odot})^{1/3}$. Therefore we can obtain the results for different M_{BH} from a single numerical result. We then numerically estimate α and β for x and y in the ranges $0.1 < x/\overline{x} < 1$ and $2 < y/x < 7$. The total number of the parameters we examined is 100 for each direction of the third body. In this section we show the main results in relation to α and β first. We will discuss the dependence of α and β on the initial direction of the third body in Sec. VI A in more detail. We will also show in Sec. VI D that the dependence of the results on the initial conditions is small.

In Fig. 1, the trajectories of the second body (the thick curve) and the third body (the dotted curve) relative to the first body are shown for (a) $x/\overline{x} = 0.3$, $y/x = 2.0$ and (b) $x/\overline{x} = 0.3$, $y/x = 4.0$. θ is chosen as $\pi/4$, where θ denotes the angle between the x-direction and the direction of the third body. The coordinate is normalized by $\overline{x}$. We see that the binary is formed through the three body interaction while the third body goes away. To see the accuracy of the numerical calculations, we checked the time reversal of the problem. That is, we have re-started the numerical integration from the final time backward to the initial time. We have found that the differences from the true values of coordinates and velocities are very small: the relative error in the coordinate position, $|\mathbf{z}_{\rm init} - \mathbf{z}(\text{time reversed})_{\rm init}|/|\mathbf{z}_{\rm init}|$, is less than 10^{-7} and the ''velocity'' component, $\mathbf{z}_{\mathbf{i}}'(\text{time reversed})$, deviates from zero by at most 10^{-5}.

Figure 2 shows the semimajor axis a as a function of initial separation $x/\overline{x}$. The solid triangles are numerical results. The solid line is the approximate equation, $a/\overline{x} = (x/\overline{x})^4$. We performed a least squares fitting of the numerical results assuming that $a/\overline{x} = \alpha(x/\overline{x})^n$. It is found that a is well fitted by the following function:

$$\frac{a}{=} \simeq 0.41\left(\frac{x}{=}\right)^{3.9}, \tag{4.1}$$

irrespective of the direction of the third body as far as we have examined ($\theta = \pi/6, \pi/4, \pi/3$). The power index n is in

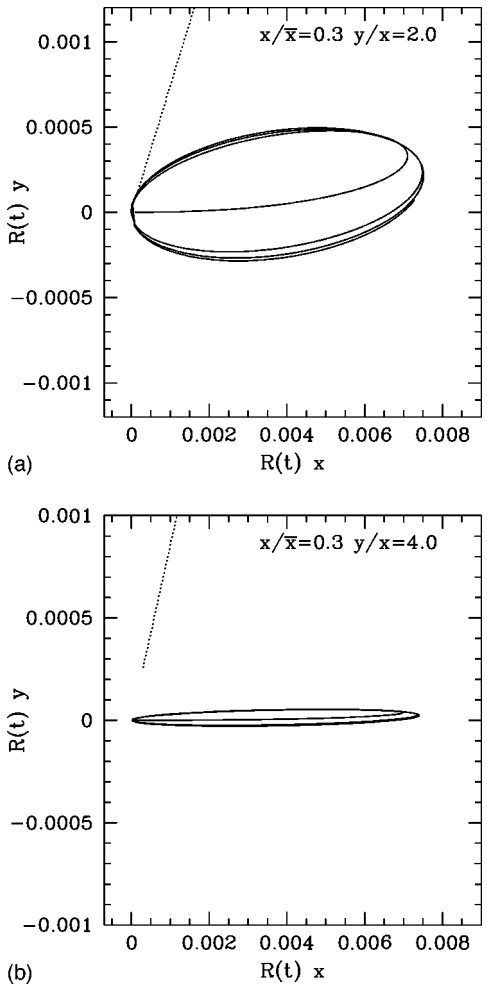

FIG. 1. The trajectories of the second body (thick curve) and the third body (dotted curve) relative to the first body for (a) $x/\bar{x}=0.3$, $y/x=2.0$ and (b) $x/\bar{x}=0.3$, $y/x=4.0$. $\theta=\pi/4$. The coordinate is normalized by $\bar{x}$.

good agreement with the analytical estimate in Eq. (2.4) so that we will not discuss the small deviation of n from 4 from now on.

Figure 3 shows b/a as a function of x/y for θ equal to (a) $\pi/6$, (b) $\pi/4$ and (c) $\pi/3$. The solid triangles are numerical results. The solid line is the approximate equation $b/a=(x/y)^3$. We see that the numerical results are parallel to the approximate estimate in a previous paper [15]. We performed a least squares fitting of the numerical results assuming that $b/a=\beta(x/y)^n$. The results are given as

$$\frac{b}{a}=0.74\left(\frac{x}{y}\right)^{3.2}\quad(\theta=\pi/6)$$

$$\frac{b}{a}=0.77\left(\frac{x}{y}\right)^{3.1}\quad(\theta=\pi/4) \tag{4.2}$$

$$\frac{b}{a}=0.62\left(\frac{x}{y}\right)^{3.1}\quad(\theta=\pi/3).$$

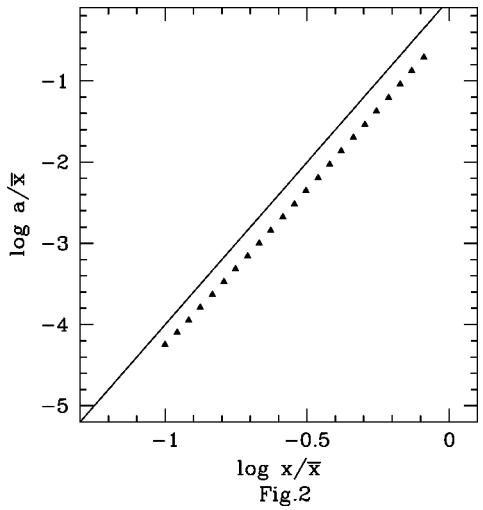

FIG. 2. The semimajor axis a as a function of initial separation $x/\bar{x}$. The solid triangles are numerical data. The solid line is the approximate equation $a/\bar{x}=(x/\bar{x})^4$.

We see a θ-dependence of β, which will be discussed in Sec. VI A. However, as for the power index n, it is almost constant so that we will not discuss the small deviation of n from 3 from now on.

The important conclusion is that we have verified that the power dependence is in good agreement with the previous analytic order-of-magnitude estimate of Eqs. (2.4) and (2.5) and that the numerical coefficients α and β are actually of order unity. In the next section we will assume that α and β are constants. For simplicity we will adopt $\alpha=0.4$ and $\beta=0.8$.

V. PROBABILITY DISTRIBUTION FUNCTION OF BINARIES

A. Distribution function and binary fraction

If we assume that black holes are distributed randomly, then the probability distribution function $P(x,y)$ for the initial comoving separation of the binary x and the initial comoving separation of the nearest neighboring black hole from the center of mass of the binary y is

$$P(x,y)dxdy=\frac{9x^2y^2}{\bar{x}^6}e^{-y^3/\bar{x}^3}dxdy, \tag{5.1}$$

where $0<x<y<\infty$ so that $\int_0^\infty dx\int_x^\infty dy P(x,y)=1$. Changing the variables x and y in Eq. (5.1) to a and e with Eqs. (2.4) and (2.6), we obtain the probability distribution function of the eccentricity and the semimajor axis of binaries as

$$f(a,e)dade=\frac{3}{4}\frac{\beta}{(\alpha\bar{x})^{3/2}}\frac{a^{1/2}e}{(1-e^2)^{3/2}}\times\exp\left[-\frac{\beta}{(1-e^2)^{1/2}}\left(\frac{a}{\alpha\bar{x}}\right)^{3/4}\right]dade, \tag{5.2}$$

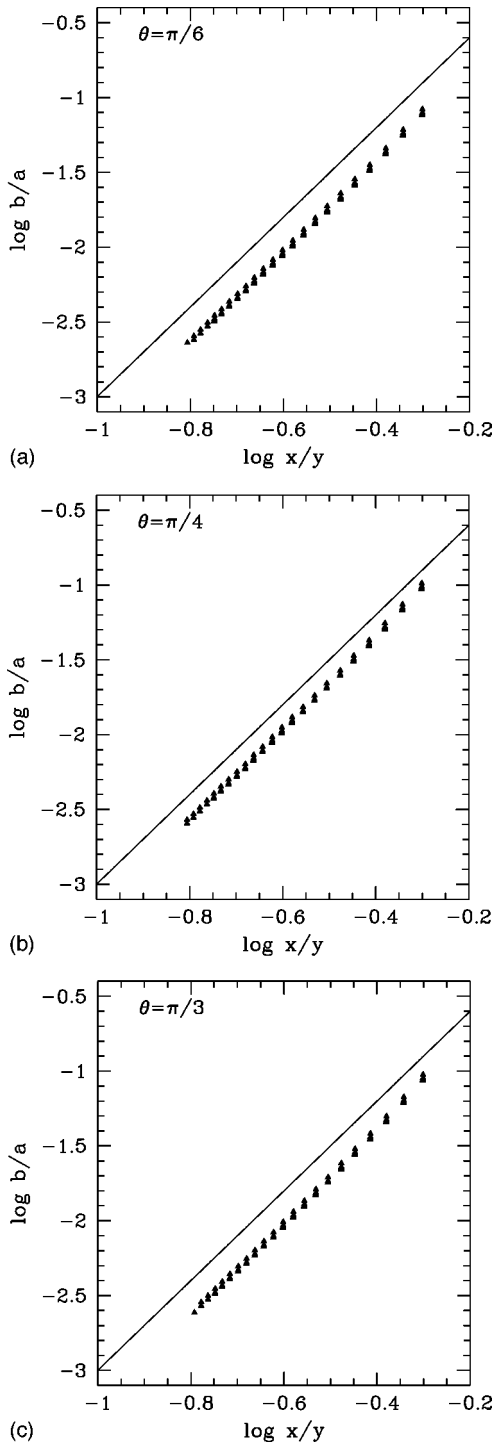

FIG. 3. b(semiminor axis)/a(semimajor axis) as a function of x/y for (a) $\theta=\pi/6$, (b) $\pi/4$ and (c) $\pi/3$. The solid triangles are numerical data. The solid line is the approximate equation $b/a=(x/y)^3$.

where $\sqrt{1-\beta^2}<e<1$, $0<a<\infty$ so that $\int_0^\infty da\int_{\sqrt{1-\beta^2}}^1 de f(a,e)=1$. For $0<e<\sqrt{1-\beta^2}$, $f(a,e)=0$: i.e., no such binary is formed.

Integrating $f(a,e)$ with respect to e in the range $\sqrt{1-\beta^2}<e<1$, we obtain the distribution function of the semimajor axis as

$$f_a(a)da=\frac{3}{4}\left(\frac{a}{\bar{\alpha x}}\right)^{3/4}\exp\left[-\left(\frac{a}{\bar{\alpha x}}\right)^{3/4}\right]\frac{da}{a}. \tag{5.3}$$

From Eq. (5.3), it is found that if $\alpha=1$, the fraction of BHMACHOs that are in binaries with $a\sim 2\times 10^{14}$ cm and $M_{BH}=0.5M_\odot$ is $\sim 4\%$ and $\sim 0.4\%$ for $\Omega h^2=1$ and 0.1, respectively. On the other hand, if we adopt our numerical estimate of α given in the previous section, $\alpha=0.4$, the fraction becomes $\sim 7\%$ and $\sim 0.8\%$ for $\Omega h^2=1$ and 0.1, respectively. This estimated fraction of ~ 10 AU size BHMACHO binaries can be compared with the observed rate of binary MACHO events (one binary event in eight observed MACHOs) [23] although the small number statistics prevents us from stating something definite.

B. Gravitational waves from coalescing BHMACHO binaries

We consider here short period BHMACHO binaries. Their coalescence time due to the emission of gravitational waves is approximately given by [24]

$$t=t_0\left(\frac{a}{a_0}\right)^4(1-e^2)^{7/2}, \tag{5.4}$$

$$a_0=2.0\times 10^{11}\left(\frac{M_{BH}}{M_\odot}\right)^{3/4}\ \text{cm} \tag{5.5}$$

where $t_0=10^{10}$ yr and a_0 is the semimajor axis of a binary with circular orbit which coalesces in t_0. Note that Eq. (5.4) is an approximation for $e\sim 1$ in Ref. [24]. However, it is also a good approximation even for $e\sim 0$. Equation (5.4) can be written in terms of x and y using Eqs. (2.4) and (2.5) as

$$t=\bar{t}\left(\frac{x}{\bar{x}}\right)^{37}\left(\frac{y}{\bar{x}}\right)^{-21}, \tag{5.6}$$

$$\bar{t}=\beta^7\left(\frac{\alpha\bar{x}}{a_0}\right)^4 t_0. \tag{5.7}$$

Integrating Eq. (5.1) for a given t with the aid of Eq. (5.6), we obtain the probability distribution function of the coalescence time $f_t(t)$. We should take the range of the integration as $0<x<\bar{x}$, $x<y<\infty$. The first condition $x<\bar{x}$ is necessary for binary formation. The second condition turns out to be $(t/\bar{t})^{1/16}\bar{x}<y<(t/\bar{t})^{-1/21}\bar{x}$ for a given t. Performing the integration, we have

$$f_t(t)dt=\frac{3}{37}\left(\frac{t}{\bar{t}}\right)^{3/37}\left[\Gamma\left(\frac{58}{37},\left(\frac{t}{\bar{t}}\right)^{3/16}\right)-\Gamma\left(\frac{58}{37},\left(\frac{t}{\bar{t}}\right)^{-1/7}\right)\right]\frac{dt}{t}$$

$$\cong\frac{3}{37}\left(\frac{t}{\bar{t}}\right)^{3/37}\Gamma\left(\frac{58}{37}\right)\frac{dt}{t}, \tag{5.8}$$

where $\Gamma(x,a)$ is the incomplete gamma function defined by

$$\Gamma(x,a)=\int_a^\infty s^{x-1}e^{-s}ds. \tag{5.9}$$

The second equality is valid when we consider $t \sim t_0$ because $t_0/\bar{t} \ll 1$ for typical values of parameters, that is, $t_0/\bar{t} \sim 2 \times 10^{-23}$ for $\Omega h^2 = 0.1$, $M_{BH} = 0.5 M_\odot$, $\alpha = 0.4$ and $\beta = 0.8$.

If the halo of our galaxy consists of BHMACHOs of mass $\sim 0.5 M_\odot$, about 10^{12} BHMACHOs exist out to the LMC. The number of coalescing binary BHMACHOs with $t \sim t_0$ then becomes $\sim 1 \times 10^9$ for $\Omega h^2 = 0.1$, $\alpha = 0.4$ and $\beta = 0.8$ so that the event rate of coalescing binaries becomes $\sim 1 \times 10^{-1}$ events/yr/galaxy. This rate is slightly larger than the estimate of Ref. [15]. On the other hand, if the BHMACHOs extend up halfway to M31, the number of coalescing binary BHMACHOs with $t \sim t_0$ can be $\sim 6 \times 10^9$ and the event rate becomes $\sim 6 \times 10^{-1}$ events/yr/galaxy. Both of these estimates are much larger than the best estimate of the event rate of coalescing neutron stars based on the statistics of binary pulsar searches in our Galaxy, $\sim 1 \times 10^{-5}$ events/yr/galaxy [25–27]. Because the first LIGO-VIRGO interferometers in 2001 should be able to detect BHMACHO coalescence out to about 15 Mpc distance, i.e., out to the Virgo Cluster [15], the event rate will be several events per year even if we pessimistically estimate it ($\sim 1/100$ events/yr/galaxy in each galaxy like our own).

In deriving the probability distribution function for the coalescence time in Eq. (5.8), we have neglected various effects, such as the angle dependence of β, 3-body collision, the effect of the fourth body, the effect of the mean fluctuation field, the initial condition dependence and the radiation drag. We will consider these effects in the next section.

C. Region checked numerically

Since we have solved three body problem only for a restricted parameter range of x and y, one may wonder whether our computations may not be complete. Thus we need to show that the parameter range of our calculations is sufficiently large.

We have verified Eqs. (2.4) and (2.5) numerically for x and y in the range $0.1\bar{x} < x < \bar{x}$, which means

$$10^{-3} < \left(\frac{x}{\bar{x}}\right)^3 < 1 \tag{5.10}$$

and $2 < y/x < 7$, which corresponds to

$$8\left(\frac{x}{\bar{x}}\right)^3 < \left(\frac{y}{\bar{x}}\right)^3 < 343\left(\frac{x}{\bar{x}}\right)^3. \tag{5.11}$$

On the other hand, y is expressed by x and t from Eq. (5.6). Therefore if we are interested in the coalescing binaries with the coalescence time $t_1 < t < t_2$, the range of y is expressed by

$$\left(\frac{t_2}{\bar{t}}\right)^{-1/7}\left[\left(\frac{x}{\bar{x}}\right)^3\right]^{37/21} < \left(\frac{y}{\bar{x}}\right)^3 < \left(\frac{t_1}{\bar{t}}\right)^{-1/7}\left[\left(\frac{x}{\bar{x}}\right)^3\right]^{37/21}. \tag{5.12}$$

This range of y determines the probability distribution function $f_t(t)$ in Eq. (5.8) for $t_1 < t < t_2$. In Fig. 4 the horizontal axis and the vertical axis are $(x/\bar{x})^3$ and $\exp[-(y/\bar{x})^3]$, respectively. The dashed lines show $x = 0.1\bar{x}$ and $y/x = \mathrm{i}$ ($\mathrm{i} = 2,3,4,5,6,7$), respectively. Solid lines show $t_1 = 0.1 t_0$ and $t_2 = 10 t_0$ for $\Omega h^2 = 0.1$, $M_{BH} = 0.5 M_\odot$, $\alpha = 0.4$ and $\beta = 0.8$ in Eq. (5.12). Since the area in Fig. 4 is directly proportional to the probability $P(x,y) = d((x/\bar{x})^3) d(e^{-(y/\bar{x})^3})$ from Eq. (5.1), almost the entire region we are interested in ($0.1 t_0 \lesssim t \lesssim 10 t_0$) is checked numerically. So the probability distribution function $f_t(t)$ in Eq. (5.8) is valid for $0.1 t_0 \lesssim t \lesssim 10 t_0$ though in deriving $f_t(t)$ we used Eqs. (2.4) and (2.5) for the region of x and y beyond our calculations.

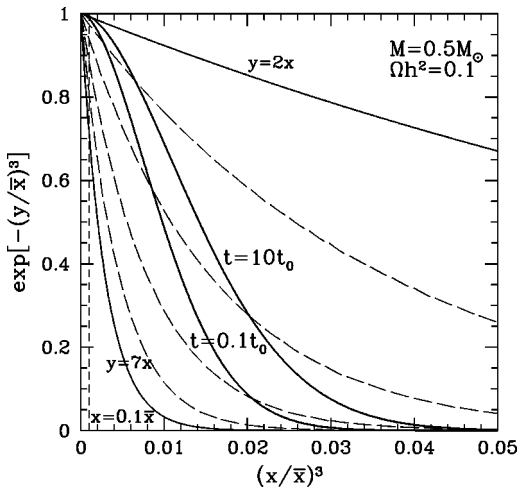

FIG. 4. The region we have checked numerically, i.e. $x = 0.1\bar{x}$ in Eq. (5.10) and $y/x = \mathrm{i}$ ($\mathrm{i} = 2,3,4,5,6,7$) in Eq. (5.11), and the region that corresponds to $0.1 t_0 < t < 10 t_0$. The horizontal axis is scaled as $(x/\bar{x})^3$ and the vertical axis is scaled as $\exp[-(y/\bar{x})^3]$ so that the area in the figure is directly proportional to the probability. We can see that almost the entire region we are interested in is within the range that we have checked numerically for $0.1 t_0 < t < 10 t_0$.

VI. CONSIDERATIONS OF VARIOUS EFFECTS

We shall consider several possible factors which may affect the estimate of the event rate of coalescence.

A. Angle dependence

So far, we have treated β as a constant. In reality, however, β has an angle dependence. In this subsection we investigate whether the angle dependence of β affects the estimate of the event rate. In the analytical estimate of Eq. (2.5), b is proportional to the tidal force. Since the tidal force is proportional to $\sin(2\theta)$, we expect that β is also proportional to $\sin(2\theta)$. In Fig. 5 we show the result of numerical calculations for the angle dependence of β averaged for various values of x and y/x for the exponent $n = 3$. We find that the angle dependence of β can be approximated by

$$\beta \simeq 0.8 \sin(2\theta). \tag{6.1}$$

In the previous section we have used the maximum value of β so that if we take this angle dependence into account the

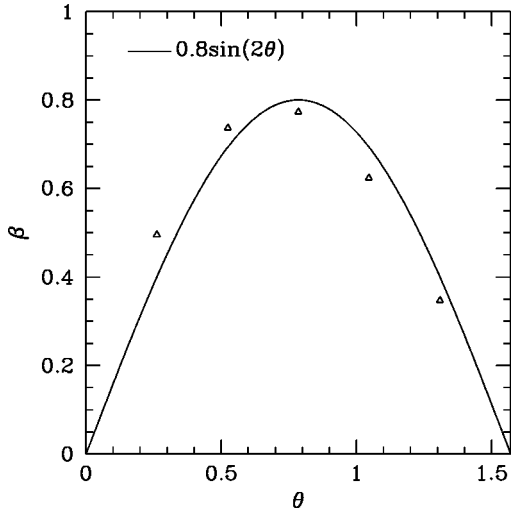

FIG. 5. The angle dependence of β assuming that the functional form of b is as in Eq. (2.5) is shown. β has an angle dependence as $\beta \propto \sin(2\theta)$. θ is the angle between the line that connects the binary and the line that connects the third body and the center of the binary.

effective β will decrease. The probability distribution function $f_t(t)$ is proportional to $\beta^{-21/37}$ since $f_t(t) \propto \bar{t}^{-3/37} \propto \beta^{-21/37}$ in Eqs. (5.8) and (5.7). Hence qualitatively the effect of the angle dependence is to increase the event rate.

If we consider the initial direction of the third body, the distribution function $P(x,y,\theta)$ for x, y and θ is given by

$$P(x,y,\theta)dxdyd\theta = P(x,y)dxdy \sin\theta d\theta = \frac{9x^2y^2}{\bar{x}^6} e^{-y^3/\bar{x}^3} dxdy \sin\theta d\theta, \tag{6.2}$$

where $0<\theta<\pi/2$ and we assumed that $P(x,y)$ does not depend on θ. Integrating Eq. (6.2) for a given t with the aid of Eq. (5.6), we obtain

$$f_t^{ang}(t)dt = \frac{3}{37} \int_{\pi/2-(1/2)\arcsin(t/\bar{t})^{1/7}}^{(1/2)\arcsin(t/\bar{t})^{1/7}} \left(\frac{t}{\bar{t}(\theta)}\right)^{3/37} \times \left[\Gamma\left(\frac{58}{37}, \left(\frac{t}{\bar{t}(\theta)}\right)^{3/16}\right) - \Gamma\left(\frac{58}{37}, \left(\frac{t}{\bar{t}(\theta)}\right)^{-1/7}\right)\right] \sin\theta d\theta \frac{dt}{t}, \tag{6.3}$$

$$\bar{t}(\theta) = \beta^7 \sin^7(2\theta) \left(\frac{\alpha\bar{x}}{a_0}\right)^4 t_0 = \bar{t} \sin^7(2\theta), \tag{6.4}$$

where β is replaced with $\beta \sin(2\theta)$. The lower and upper limits of the θ integral are determined by $t/\bar{t}(\theta)=1$ where the integrand in Eq. (6.3) becomes 0; i.e., no binary which survives up to $t \sim t_0$ is produced. We can integrate Eq. (6.3) numerically with respect to θ for a given t. For example, if we take $t=t_0$, $M_{BH}=0.5M_\odot$, $\Omega h^2=0.1$, $\alpha=0.4$ and $\beta=0.8$, then $f_t^{ang}(t_0)=1.8\times10^{-3}/t_0$ while $f_t(t_0)=1.0\times10^{-3}/t_0$. For $0.1t_0 \lesssim t \lesssim 10t_0$, we can show that $f_t^{ang}(t_0) > f_t(t_0)$. Therefore the event rate of coalescing binaries may be doubled if we take into account the angle dependence of β.

B. Three-body collision

In deriving Eq. (5.8), we take the range of the integration as $0<x<\bar{x}$, $x<y<\infty$. Here we consider the range of y carefully. If $y<\bar{x}$, the third body may be bound by the binary in the radiation dominated era. If the bound third body collides with the binary, a complicated 3-body interaction occurs. It is a difficult problem to estimate how many binaries whose coalescence time is $\sim t_0$ are left after the complicated 3-body interaction. So we shall exclude such a case and estimate the minimum event rate. Namely, we shall restrict the range of the integration to $0<x<\bar{x}$, $\bar{x}<y<\infty$.[1] This range turns out to be $\bar{x}<y<(t/\bar{t})^{-1/21}\bar{x}$ for a given t. Integrating Eq. (5.1) for a given t with the aid of Eq. (5.6), we have

$$f_t^{3\ body}(t)dt = \frac{3}{37}\left(\frac{t}{\bar{t}}\right)^{3/37}\left[\Gamma\left(\frac{58}{37},1\right) - \Gamma\left(\frac{58}{37}, \left(\frac{t}{\bar{t}}\right)^{-1/7}\right)\right]\frac{dt}{t} \cong \frac{3}{37}\left(\frac{t}{\bar{t}}\right)^{3/37}\Gamma\left(\frac{58}{37},1\right)\frac{dt}{t}. \tag{6.5}$$

The second equality is valid when we consider $t \sim t_0$. Its ratio to $f_t(t)$ in Eq. (5.8) is

$$\frac{f_t^{3\ body}(t)}{f_t(t)} = \frac{\Gamma(58/37,1)}{\Gamma(58/37)} \simeq 0.60. \tag{6.6}$$

That is, the ratio of the binary formation probability without the third body being bound by the binary to the total binary formation probability is about 60% for $t \sim t_0$. Hence the 3-body collision reduces the event rate at most 40%.

If we consider the fourth body, the bound third body may not collide directly with the binary due to the tidal force of the fourth body to the third body. The third body may only act as a satellite of the binary. If this fact is taken into account, the minimum probability distribution function $f_t^{3\ body}(t)$ in Eq. (6.5) increases. The semimajor axis a' and the semiminor axis b' of the orbit of the third body will be determined by the initial comoving separation of the fourth body z as

[1]The factor in front of $\bar{x}$ in the condition $\bar{x}<y$ may be more than unity for the third body not to be bound in this case, since the binary is more massive than a single black hole. However, we set it unity from now on, since the factor is of order $O(1)$ and the conclusion that the event rate of coalescing binaries is not reduced so much is not changed. This statement also applies to Eq. (6.12).

$$a' = \alpha' \frac{y^4}{\overline{x^3}} \tag{6.7}$$

and

$$b' = \beta' \left(\frac{y}{z}\right)^3 a' \tag{6.8}$$

respectively. In deriving these values, we treat the binary as a point mass and assume that the analytical estimates of Eqs. (2.4) and (2.5) are valid for this system. α' and β' will be different from α and β respectively in this case, since the mass ratio of the total mass of the binary to the third body's mass is not unity. However, we set $\alpha' = \alpha$ and $\beta' = \beta$ from now on for simplicity since we are making an order estimate of the effect.

The 3-body collision will not occur when $\gamma a < r'_{min}$ is satisfied, where γ is a constant which takes into account the uncertainty of the criterion for the 3-body collision. r'_{min} is the minimum separation between the third body and the center of mass of the binary and is given by

$$r'_{min} = a'(1-e') = a' - \sqrt{a'^2 - b'^2} \gtrsim \frac{b'^2}{2a'}. \tag{6.9}$$

The third inequality is almost an equality because the case with $a' \gg b'$ is considered. The distribution function of four bodies is given by

$$P_{x,y,z}(x,y,z)dxdydz = \frac{27}{\overline{x^9}} e^{-z^3/\overline{x^3}} x^2 dx y^2 dy z^2 dz. \tag{6.10}$$

To calculate the probability that the third body does not collide with the binary but is bound to it, the above distribution function, Eq. (6.10), should be integrated with the constraints

$$x < y < \overline{x}, \tag{6.11}$$

$$\overline{x} < z, \tag{6.12}$$

$$z^3 < \delta \frac{y^5}{x^2}, \tag{6.13}$$

where $\delta = \sqrt{\beta^2/2\gamma}$ and the last inequality comes from $\gamma a < r'_{min}$. The condition (6.12) is necessary in order that the fourth body is not bound in the radiation dominated era. First, we integrate Eq. (6.10) with respect to z as

$$\int_1^{\delta(y/\overline{x})^5/(x/\overline{x})^2} e^{-(z/\overline{x})^3} d\left(\frac{x^3}{\overline{x^3}}\right) d\left(\frac{y^3}{\overline{x^3}}\right) d\left(\frac{z^3}{\overline{x^3}}\right) = \left[e^{-1} - e^{-\delta(y/\overline{x})^5/(x/\overline{x})^2}\right] d\left(\frac{x^3}{\overline{x^3}}\right) d\left(\frac{y^3}{\overline{x^3}}\right), \tag{6.14}$$

where the range of the z integral is determined by Eqs. (6.12) and (6.13). The first term in Eq. (6.14) can be integrated for a given t with the aid of Eq. (5.6) as

$$\begin{aligned}\int_{[(x/\overline{x})^{37}(y/\overline{x})^{-21} = t/\overline{t}]} e^{-1} d\left(\frac{x^3}{\overline{x^3}}\right) d\left(\frac{y^3}{\overline{x^3}}\right) &= \left\{ \int_{\delta^{-111/143}(t/\overline{t})^{6/143}}^1 e^{-1} \left(\frac{y^3}{\overline{x^3}}\right)^{21/37} d\left(\frac{y^3}{\overline{x^3}}\right) \right\} d\left(\left(\frac{t}{\overline{t}}\right)^{3/37}\right) \\ &= \frac{3}{37}\left(\frac{t}{\overline{t}}\right)^{3/37} \left\{ \frac{37}{58e}\left[1 - \delta^{-174/143}\left(\frac{t}{\overline{t}}\right)^{348/5291}\right]\right\} \frac{dt}{t}.\end{aligned} \tag{6.15}$$

The upper limit of this integral is determined by Eq. (6.11), and the lower limit is determined by Eq. (5.6) and $\overline{x^3} < \delta y^5/x^2$ with Eqs. (6.12) and (6.13). The second term in Eq. (6.14) can be integrated in the same way.

On the other hand, the probability distribution function of the binary formation without the third body being bound by the binary is already obtained in Eq. (6.5). Then, by summing the case with the third body being bound by the binary and the case without the third body being bound by the binary, the probability distribution function without the collision between the third body and the binary is obtained as

$$\begin{aligned} f_t^{4\ body}(t)dt &= f_t^{3\ body}(t)dt + \frac{3}{37}\left(\frac{t}{\overline{t}}\right)^{3/37} \left\{ \frac{37}{58e}\left[1 - \delta^{-174/143}\left(\frac{t}{\overline{t}}\right)^{348/5291}\right] \right. \\ &\quad \left. - \frac{111}{143}\delta^{-174/143}\left(\frac{t}{\overline{t}}\right)^{348/5291}\left[\Gamma\left(\frac{174}{143},1\right) - \Gamma\left(\frac{174}{143},\delta\left(\frac{t}{\overline{t}}\right)^{-2/37}\right)\right]\right\} \frac{dt}{t} \\ &\cong f_t^{3\ body}(t)dt + f_t(t)\left[\frac{37}{58e\Gamma\left(\frac{58}{37}\right)}\right] dt. \end{aligned} \tag{6.16}$$

The relative error in the second equality is about a few percent for $t\sim t_0$ and $\gamma\sim 1$. The second term is the probability distribution function for the third body to be bound by the binary but not to collide with the binary. For simplicity, we set $\gamma=1$, which corresponds to $\delta\cong 0.57$ for $\beta=0.8$. The ratio $f_t^{4\ body}(t_0)/f_t(t_0)$ is 82% for $M_{BH}=0.5M_\odot$, $\Omega h^2=0.1$, $\alpha=0.4$ and $\beta=0.8$. Comparing this ratio to the ratio in Eq. (6.6), the hierarchical three body bound system may be produced by about 22% of the binaries that coalesce at $t\sim t_0$, during the radiation dominated era. During the radiation dominated era, the probability of the 3-body collision is about 18% of the binaries that coalesce at $t\sim t_0$.

Because the hierarchical structure consisting of a binary and a satellite becomes unstable by $t\sim t_0$ if r'_{min}/a is very close to 1, we may have to take γ larger than unity. Moreover, γ will depend on the eccentricity of the binary, the inclination of the orbital plane of the third body and so on. Here ''unstable'' means that the third body crosses the binary and the complicated three body interaction occurs. There are some criterions for the stability of the binary (e.g. Ref. [28]). If we need to estimate the event rate accurately, we will have to pay attention to the value of γ. However, we do not need such an accuracy here, and so we set γ as a constant. For $\gamma=10$, the ratio $f_t^{4\ body}(t_0)/f_t(t_0)$ is 71% for $M_{BH}=0.5M_\odot$, $\Omega h^2=0.1$, $\alpha=0.4$ and $\beta=0.8$.

In addition to the stability of the hierarchical system, there may be something to be considered about the value of γ. If the third body is not separated enough from the binary, the tidal force from the third body deforms the orbit of the binary more effectively than the gravitational wave does. Then the estimate of the lifetime of the binary using Eq. (5.4) is not adequate for $t\sim t_0$, which results in a change of the event rate estimate. Note that a little change in the eccentricity, e, causes a large change in the lifetime in Eq. (5.4) when the orbit is very eccentric, $1-e^2\ll 1$. The effect of the orbital deformation will be discussed in Sec. VII.

C. Effect of mean fluctuation field

In this subsection, we will estimate the tidal force from bodies other than the third body and how it affects the estimate of the event rate. The tidal field from the ith BH will be given by

$$T_i\propto\frac{1}{x_i^3}, \tag{6.17}$$

where x_i is the comoving separation of the ith BHMACHO from the center of mass of the binary. The distribution function for $x_4,x_5,\ldots,x_i$ is

$$P(x_4,x_5,\ldots,x_i)=e^{-x_i^3/\overline{x^3}}d\left(\frac{x_4^3}{\overline{x^3}}\right)d\left(\frac{x_5^3}{\overline{x^3}}\right)\cdots d\left(\frac{x_i^3}{\overline{x^3}}\right). \tag{6.18}$$

Then the mean value of $(1/x_i^3)^2$ for given x_3 is estimated as

$$\left\langle\frac{1}{x_i^6}\right\rangle=\frac{\int_{x_3^3/\overline{x^3}}^\infty d(x_4^3/\overline{x^3})\int_{x_4^3/\overline{x^3}}^\infty d(x_5^3/\overline{x^3})\cdots\int_{x_{i-1}^3/\overline{x^3}}^\infty d(x_i^3/\overline{x^3})e^{-x_i^3/\overline{x^3}}(1/x_i^6)}{\int_{x_3^3/\overline{x^3}}^\infty d(x/4^3/\overline{x^3})\int_{x_4^3/\overline{x^3}}^\infty d(x_5^3/\overline{x^3})\cdots\int_{x_{i-1}^3/\overline{x^3}}^\infty d(x_i^3/\overline{x^3})e^{-x_i^3/\overline{x^3}}}$$

$$=\frac{1}{\overline{x^6}}\int_f^\infty dv_4\int_{v_4}^\infty dv_5\cdots\int_{v_{i-2}}^\infty dv_{i-1}\int_{v_{i-1}}^\infty\frac{dv_i}{v_i^2}e^{-v_i}/e^{-f}, \tag{6.19}$$

where

$$f\equiv\frac{x_3^3}{\overline{x^3}}. \tag{6.20}$$

Thus the mean value of the tidal field for given x_3 will be estimated as

$$\langle T^2\rangle=N\sum_{i=3}^\infty\left\langle\frac{1}{x_i^6}\right\rangle$$

$$=\frac{N}{x_3^6}\left[1+f^2\sum_{i=4}^\infty\int_f^\infty dv_4\int_{v_4}^\infty dv_5\cdots\right.$$

$$\left.\times\int_{v_{i-2}}^\infty dv_{i-1}\int_{v_{i-1}}^\infty\frac{dv_i}{v_i^2}e^{-v_i+f}\right]. \tag{6.21}$$

The first term is the contribution from the third object and the second term is that from the other objects.

For $i\geqslant 5$,

$$I_i\equiv e^f\int_f^\infty dv_4\int_{v_4}^\infty dv_5\cdots\int_{v_{i-2}}^\infty dv_{i-1}\int_{v_{i-1}}^\infty\frac{dv_i}{v_i^2}e^{-v_i}$$

$$=e^f\int_f^\infty dv_4\int_{v_4}^\infty dv_5\cdots\int_{v_{i-2}}^\infty\frac{dv_{i-1}}{v_{i-1}}\int_1^\infty\frac{dx}{x^2}e^{-v_{i-1}x}$$

$$=e^f\int_f^\infty dv_4\int_{v_4}^\infty dv_5\cdots\int_1^\infty\frac{dy}{y}\int_1^\infty\frac{dx}{x^2}e^{-v_{i-2}xy}$$

$$=e^f\int_1^\infty\frac{dy}{y^{i-4}}\int_1^\infty\frac{dx}{x^{i-3}}e^{-fxy}. \tag{6.22}$$

Thus

$$\begin{aligned}\tilde{I} &:= \sum_{i=5}^{\infty} I_i \\ &= e^f \int_1^\infty dy \int_1^\infty \frac{dx}{x} \frac{1}{xy-1} e^{-fxy} \\ &= e^f \int_1^\infty dy y' \int_y^\infty dz \frac{1}{z(z-1)} e^{-fz} \\ &= e^f \left[-\int_1^\infty dz \frac{1}{z(z-1)} e^{-fz} + \int_1^\infty dz \frac{1}{z-1} e^{-fz} \right] \\ &= e^f \mathrm{Ei}(-f). \end{aligned} \tag{6.23}$$

On the other hand, for $i=4$,

$$\begin{aligned} I_4 &:= e^f \int_f^\infty \frac{dv_4}{v_4^2} e^{-v_4} = e^f \left(f^{-1} e^{-f} - \int_f^\infty \frac{dv}{v} e^{-v} \right) \\ &= f^{-1} - e^f \mathrm{Ei}(-f). \end{aligned} \tag{6.24}$$

Hence

$$\begin{aligned} I &:= \sum_{i=4}^{\infty} \int_f^\infty dv_4 \int_{v_4}^\infty dv_5 \cdots \int_{v_{i-2}}^\infty dv_{i-1} \int_{v_{i-1}}^\infty \frac{dv_i}{v_i^2} e^{-v_i + f} \\ &= I_4 + \tilde{I} = f^{-1} \end{aligned} \tag{6.25}$$

Therefore (tidal force by the fourth, fifth, ... objects)/(tidal force by the third object) is estimated as $\sim f$. Note that this averaged value of the tidal force by the fourth, fifth, ... objects can be evaluated more easily. Because the distribution is assumed to be random in space, the one particle distribution function for the fourth, fifth, ... objects is given by a uniform distribution in $x > x_3$ with the averaged density of the BHMACHOs. Hence

$$\sum_{i=4}^{\infty} \left\langle \frac{1}{x_i^6} \right\rangle = \frac{3}{4\pi \bar{x}^3} \int_{x_3}^\infty \frac{1}{x^6} 4\pi x^2 dx = \frac{1}{x_3^3 \bar{x}^3}.$$

Of course, this gives the same result as before.

If $y > \bar{x}$, i.e. $f > 1$, the tidal force by the fourth, fifth, ... objects dominates the one by the third body. In deriving $f_t(t)$ in Eq. (5.8) or $f_t^{3\ body}(t)$ in Eq. (6.5), we should take the effect of the fluctuation field into consideration. If the tidal force increases, β increases effectively; eventually $f_t(t)$ and $f_t^{3\ body}(t)$ decrease because $f_t(t)$ and $f_t^{3\ body}(t) \propto \bar{t}^{-3/37} \propto \beta^{-21/37}$. To estimate how the minimum event rate decreases, we use

$$\langle T^2 \rangle = \frac{N}{x_3^6} \left[1 + \left(\frac{x_3}{\bar{x}} \right)^3 \right] \lesssim \frac{N}{x_3^6} \left[2 \left(\frac{x_3}{\bar{x}} \right)^3 \right] \tag{6.26}$$

as the tidal force for $y > \bar{x}$. Assuming that the analytical estimate, $b \simeq$ (tidal force) $\times$ (free fall time)^2, is valid as in Eq. (2.5), we have

$$b = \sqrt{2} \beta \left(\frac{x}{y} \right)^3 \left(\frac{y}{\bar{x}} \right)^{3/2} a. \tag{6.27}$$

With this equation and Eq. (2.4), assuming that the form of a in Eq. (2.4) is valid, we write Eq. (5.4) in terms of x and y as

$$t = 2^{7/2} \bar{t} \left(\frac{x}{\bar{x}} \right)^{37} \left(\frac{y}{\bar{x}} \right)^{-21/2}. \tag{6.28}$$

We take the range of the integration as $0 < x < \bar{x}$, $\bar{x} < y < \infty$ which means that we exclude the case that the third body is bound to the binary. Integrating Eq. (5.1) for a given t with the aid of Eq. (6.28) in the range of $\bar{x} < y < 2^{1/3} (t/\bar{t})^{-2/21} \bar{x}$, we have

$$\begin{aligned} & f_t^{fluc}(t) dt \\ &= \frac{3}{37} \left(\frac{t}{\bar{t}} \right)^{3/37} 2^{-21/74} \left[\Gamma\left(\frac{95}{74}, 1 \right) - \Gamma\left(\frac{95}{74}, 2 \left(\frac{t}{\bar{t}} \right)^{-2/7} \right) \right] \frac{dt}{t} \\ &\cong \frac{3}{37} \left(\frac{t}{\bar{t}} \right)^{3/37} 2^{-21/74} \Gamma\left(\frac{95}{74}, 1 \right) \frac{dt}{t}. \end{aligned} \tag{6.29}$$

The ratio of $f_t^{fluc}(t)$ in Eq. (6.29) to $f_t(t)$ in Eq. (5.8) is

$$\frac{f_t^{fluc}(t)}{f_t(t)} = \frac{2^{-21/74} \Gamma(95/74, 1)}{\Gamma(58/37)} \simeq 0.40. \tag{6.30}$$

Hence the tidal force from bodies other than the third body reduces the event rate at most 60%.[2]

D. Initial condition dependence

So far we have assumed that the initial peculiar velocity is vanishing and the initial scale factor when the bodies begin to interact is $R = 10^{-3} (x/\bar{x}) (M_{BH}/0.5 M_\odot)^{1/3}$. We consider here whether or not the results crucially depend on the initial conditions.

First, we consider the initial angular momentum. We have assumed that the angular momentum of the binary is only from the tidal force so that it is given by

$$J = b \sqrt{\frac{M_{BH}^3}{2a}} = \sqrt{\frac{\alpha \beta^2}{2}} M_{BH}^3 \frac{x^{10}}{y^6 \bar{x}^3}, \tag{6.31}$$

where we used Eqs. (2.4) and (2.5). On the other hand, if the BHMACHO binary has a relative velocity v_f at the formation epoch, the initial angular momentum will be evaluated as

$$J_f = M_{BH} R_f x v_f, \tag{6.32}$$

[2] In $f_t^{fluc}(t)$, the case where the third body is bound to the binary is excluded. So we will have to compare it with $f_t^{3\ body}(t)$ not with $f_t(t)$ to evaluate only the effect of the mean fluctuation field: $f_t^{fluc}(t)/f_t^{3\ body}(t) = 0.67$.

where R_f is given by Eq. (2.1). We note that $v_f<1$. Otherwise, the BHMACHO mass becomes comparable with the radiation energy within the volume that the BHMACHO sweeps in one Hubble expansion time at the formation epoch. In this case the drag effect due to the radiation field will be significant so that the BHMACHO will be decelerated eventually and $v_f<1$ after all. We can now evaluate the ratio of the two angular momenta as

$$\left|\frac{J_f}{J}\right| \simeq 9\times10^{-3} v_f \left(\frac{M_{BH}}{M_\odot}\right)^{1/6} (\Omega h^2)^{1/3} \left(\frac{x}{\bar{x}}\right)^{-4} \left(\frac{y}{\bar{x}}\right)^{3}$$
$$< 4\times10^{-3} \left(\frac{x}{\bar{x}}\right)^{-4} \left(\frac{y}{\bar{x}}\right)^{3}$$
$$= 4\times10^{-3} \left(\frac{t}{\bar{t}}\right)^{-1/7} \left(\frac{x}{\bar{x}}\right)^{9/7} < 4\times10^{-3} \left(\frac{t}{\bar{t}}\right)^{-1/7}, \tag{6.33}$$

where we used Eqs. (2.1), (2.2) and (5.6) for $M_{BH}=0.5M_\odot$, $\Omega h^2=0.1$, $\alpha=0.4$ and $\beta=0.8$. For $t\sim t_0$, $|J_f/J|$ can be comparable to 7 for the extreme case of $v_f\sim1$ since $t_0/\bar{t}\sim2\times10^{-23}$. Because $f_t(t)\propto\beta^{-21/37}$, the event rate becomes 30% of Eq. (5.8) if the initial peculiar velocity is the maximum possible value. Hence we see that the event rate is not reduced so much even if the initial peculiar velocity is extremely large.

Second, we consider whether the initial peculiar velocity considerably changes α and the formation epoch of the binary. Consider the case that the initial peculiar velocity is comparable to unity when $R=R_f\sim10^{-9}$ in Eq. (2.1) for $M_{BH}\sim0.5M_\odot$ and $\Omega h^2\sim0.1$. From Eq. (3.5), the peculiar velocity is damped to $\sim10^{-6}(x/\bar{x})^{-1}$ by the time when $R=10^{-3}(x/\bar{x})$, since the interaction between bodies can be neglected during this period. Therefore it is sufficient to investigate the two body problem assuming that the peculiar velocity v_i is smaller than $10^{-6}(x/\bar{x})^{-1}$ at $R=10^{-3}(x/\bar{x})$. The result is shown in Fig. 6. Figure 6 shows that α and the formation epoch of the binary do not crucially depend on the initial peculiar velocity. When $v_i=-10^{-6}(x/\bar{x})^{-1}$, the event rate changes because $f_t(t)\propto\bar{t}^{-3/37}\propto\alpha^{-12/37}$. Since α is about 10% larger, the event rate is only 4% smaller. Note that the ratio $R\dot{x}/\dot{R}x\sim10^{-3}v_i(x/\bar{x})^{-1}$ does not depend on R.

Finally, we consider whether the initial scale factor changes α and the formation epoch of the binary. We calculated the two body problem using various initial scale factors. The results are shown in Fig. 7. As we can see from Fig. 7, α and the formation epoch of the binary do not strongly depend on the initial scale factor. Qualitatively the event rate increases if the interaction begins earlier than $R=10^{-3}x/\bar{x}$, because α decreases.

E. Radiation drag

In this subsection we consider whether or not the force received from the background radiation is greater than the gravitational force between BHMACHOs. There are two kinds of force received from the background radiation: (i) the force from the radiation through which a BHMACHO is traveling [29] and (ii) the force from the radiation which a BHMACHO deflects, namely the dynamical friction [30,31].

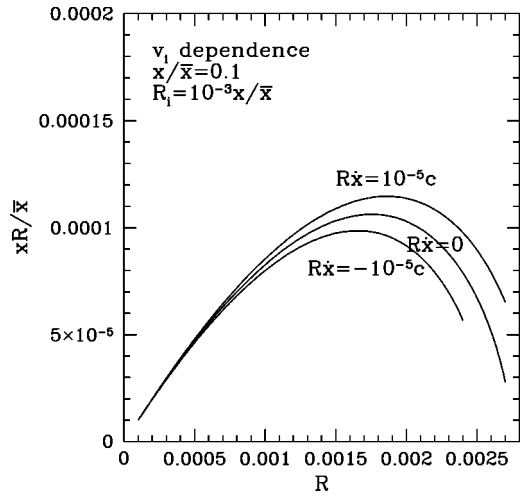

FIG. 6. This figure illustrates whether the initial peculiar velocity crucially changes α or the formation epoch of the binary. The evolution of the relative distance between the binary with different initial peculiar velocity at $R_i=10^{-3}(x/\bar{x})$ is shown. The case of $v_i=10^{-6}(x/\bar{x})^{-1}$ is the upper one. The case of $v_i=0$ is the middle one. The case of $v_i=-10^{-6}(x/\bar{x})^{-1}$ is the lower one. We can see that the dependence is weak.

First, we estimate the force from the radiation which the BHMACHO sweeps. The force is estimated as

$$F_{rad}\sim(\text{radiation momentum density})$$
$$\times(\text{cross section})\times(\text{velocity of the BH})$$
$$\sim\frac{\rho_{eq}}{R^4}\times M_{BH}^2\times v. \tag{6.34}$$

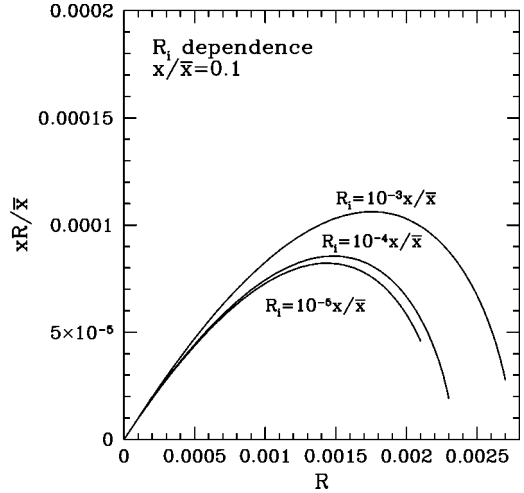

FIG. 7. This illustrates whether the initial scale factor when the bodies begin to interact crucially changes α or the formation epoch of the binary. The cases of $R_i=10^{-3}(x/\bar{x})$, $R_i=10^{-4}(x/\bar{x})$ and $R_i=10^{-5}(x/\bar{x})$ are shown. We can see that the dependence is weak.

When $R \simeq R_m$, the ratio of the force from the radiation to the gravitational force between BHMACHOs is

$$\frac{F_{rad}}{F_{grav}} \simeq \frac{M_{BH}^2 v \rho_{eq}/R_m^4}{M_{BH}^2/(xR_m)^2} \sim 10^{-11}\left(\frac{M_{BH}}{M_\odot}\right)^{2/3}(\Omega h^2)^{4/3} v \left(\frac{x}{\bar{x}}\right)^{-4} \lesssim 10^{-13}\left(\frac{x}{\bar{x}}\right)^{-4} \tag{6.35}$$

where we set $M_{BH}=0.5M_\odot$ and $\Omega h^2=0.1$. Therefore the force from the radiation which the BHMACHO sweeps can be neglected for $x/\bar{x} \gtrsim 10^{-3}$. Since our numerical calculations are performed for $x/\bar{x}>0.1$, the radiation drag force is negligible.

Next, we investigate whether the dynamical friction can be larger than the gravitational force between the BHMACHOs. When a photon passes by a BHMACHO at a distance b, the photon is deflected by an angle $\theta_d \sim 4M_{BH}/b$. This deflection changes the momentum direction of the photon. The momentum of the photon in the incoming direction changes from p to $p(1-\cos\theta_d)$. Thus the momentum of the BHMACHO must be changed. This momentum exchange causes the dynamical friction. The force that the BHMACHO receives due to the dynamical friction can be estimated as

$$F_{dyn} = \int (\text{radiation momentum density}) \times (\text{velocity of the BH}) \times (1-\cos\theta_d) 2\pi b db. \tag{6.36}$$

This expression may not be precise relativistically, but this will be a good approximation when $v \ll 1$. Assuming θ_d is small,

$$F_{dyn} \simeq \int_{b_{min}}^{b_{max}} \frac{\rho_{eq}}{R^4} v \theta_d^2 b db \simeq \frac{\rho_{eq}}{R^4} M_{BH}^2 v \ln\Lambda, \tag{6.37}$$

where $\ln\Lambda = \ln b_{max}/b_{min}$ is called the Coulomb logarithm. $b_{max}(b_{min})$ is the maximum (minimum) of the impact parameter. In the cosmological situation the horizon scale sets the natural maximum impact parameter. In the case we are considering, $b_{min} \simeq M_{BH}$. Therefore $\ln\Lambda$ cannot be so large, and F_{dyn} is the same order as F_{rad}. Hence the dynamical friction can also be neglected.

VII. LIFE OF BHMACHO BINARIES AFTER FORMATION

Finally, we consider how BHMACHO binaries evolve after the equality time.

First, we consider a 3-body collision during the matter dominated era. For example, let us consider a galaxy with mass $M_G \sim 10^{12} M_\odot$ and a radius $R_G \sim 100$ kpc. Then the density of BHMACHOs n is about $n \sim 1/(10^{19}\ \text{cm})^3$. We estimate the time scale t_{coll} for a BHMACHO binary with the semimajor axis $a \sim 2\times 10^{15}$ cm (which corresponds to $x/\bar{x} \sim 0.4$) to collide with other BHMACHOs. Note that almost all binaries that contribute to the event rate have $x/\bar{x} \lesssim 0.4$ as we can see in Fig. 4. If we assume the velocity of the binary v to be the virial velocity $v \sim \sqrt{M_G/R_G} \sim 100$ km/s, t_{coll} is given by

$$t_{coll} \sim \frac{1}{n\sigma v} \sim 10^{12}\ \text{yr} \gg 10^{10}\ \text{yr}, \tag{7.1}$$

where $\sigma \sim \pi a^2 \sim 10^{31}\ \text{cm}^2$ is the cross section for the 3-body collision. Hence the 3-body collision during the matter dominated era may be small.

Next, we consider whether or not the tidal force from the other BHMACHOs alters the coalescence time of the binary. If the tidal field from the other bodies deforms the orbit of the binary more effectively than the gravitational wave does, the lifetime of the binary in Eq. (5.4) may be different. For example, the binary cannot coalesce if the increase of the binding energy by the tidal force is greater than the decrease by the gravitational wave emission. Since the binaries that contribute to the coalescence rate at present are highly eccentric, $1-e^2 \ll 1$, a little change in the eccentricity, e, causes a large change in the lifetime in Eq. (5.4). If the coalescence time of the binary in Eq. (5.4) is different, the probability distribution function for the coalescence time $f_t(t)$ in Eq. (5.8) is different since we use Eq. (5.4) in deriving $f_t(t)$, and the event rate of the coalescing BHMACHO binaries may be reduced.

So let us consider the tidal field from the other bodies on the orbit of the binary after the equality time. First, we compare the energy loss rate by the gravitational wave with the binding energy change rate by the tidal field from the other bodies. The average energy loss rate by the gravitational wave [24] from a binary with the eccentricity e and the semimajor axis a is given by

$$|\dot{E}^{(GW)}| = \frac{64 M_{BH}^5\left(1+\frac{73}{24}e^2+\frac{37}{96}e^4\right)}{5a^5(1-e^2)^{7/2}}. \tag{7.2}$$

On the other hand, the energy change rate by the tidal force from the other body is at most given as

$$|\dot{E}^{(tidal)}| \sim (\text{tidal force}) \times (\text{velocity}) \sim \frac{M_{BH}^2 a}{D^3} \times \frac{2a}{T_B}, \tag{7.3}$$

where $T_B = 2\pi\sqrt{a^3/2M_{BH}}$ is the period of the binary and D is the distance between the source of the tidal force and the center of mass of the binary. The ratio is

$$|\dot{E}^{(GW)}/\dot{E}^{(tidal)}| \sim \left(\frac{D}{2\times10^{25}\ \mathrm{cm}}\right)^3 \left(\frac{x}{\bar{x}}\right)^{-43} \left(\frac{y}{\bar{x}}\right)^{21} \left(\frac{M_{BH}}{0.5M_\odot}\right)^{-11/6} \left(\frac{\Omega h^2}{0.1}\right)^{22/3}$$
$$\sim \left(\frac{D}{2\times10^{25}\ \mathrm{cm}}\right)^3 \left(\frac{t}{\bar{t}}\right)^{-1} \left(\frac{x}{\bar{x}}\right)^{-6} \left(\frac{M_{BH}}{0.5M_\odot}\right)^{-11/6} \left(\frac{\Omega h^2}{0.1}\right)^{22/3}$$
$$\sim \left(\frac{D}{1\times10^{17}\ \mathrm{cm}}\right)^3 \left(\frac{x/\bar{x}}{0.4}\right)^{-6} \left(\frac{M_{BH}}{0.5M_\odot}\right)^{-21/6} \left(\frac{\Omega h^2}{0.1}\right)^{2}, \tag{7.4}$$

where we used Eqs. (2.4) and (2.6) with $\alpha=0.4$, $\beta=0.8$ and $e\sim1$ in the first equality. We used Eq. (5.6) in the second equality and we set $t=t_0$ in the third equality. Therefore if $D>1\times10^{17}$ cm, the coalescence time based on Eq. (5.4) is a good approximation for a binary with the semimajor axis $a\lesssim2\times10^{15}$ cm, which corresponds to $x/\bar{x}\lesssim0.4$, since $|\dot{E}^{(GW)}/\dot{E}^{(tidal)}|>1$. This condition is satisfied in our case since the mean separation of BHMACHOs is $\sim2\times10^{17}$ cm at the equality time.

Second, we compare the angular momentum loss rate by the gravitational wave with that by the tidal field of the other body. The average angular momentum loss rate by the gravitational wave [24] for a binary with eccentricity e and semimajor axis a is given by

$$|\dot{J}^{(GW)}| = \frac{32\sqrt{2}M_{BH}^{9/2}\left(1+\frac{7}{8}e^2\right)}{5a^{7/2}(1-e^2)^2}. \tag{7.5}$$

On the other hand, the average rate of the angular momentum change by the tidal field is at most given as

$$|\dot{J}^{(tidal)}| \sim (\text{tidal force})\times(\text{length}) \sim \frac{M_{BH}^2a^2}{D^3}. \tag{7.6}$$

Their ratio is calculated as

$$|\dot{J}^{(GW)}/\dot{J}^{(tidal)}| \sim \left(\frac{D}{2\times10^{26}\ \mathrm{cm}}\right)^3 \left(\frac{x}{\bar{x}}\right)^{-34} \left(\frac{y}{\bar{x}}\right)^{12} \left(\frac{M_{BH}}{0.5M_\odot}\right)^{2/3} \left(\frac{\Omega h^2}{0.1}\right)^{22/3}$$
$$\sim \left(\frac{D}{2\times10^{26}\ \mathrm{cm}}\right)^3 \left(\frac{t}{\bar{t}}\right)^{-12/21} \left(\frac{x}{\bar{x}}\right)^{-90/7} \left(\frac{M_{BH}}{0.5M_\odot}\right)^{2/3} \left(\frac{\Omega h^2}{0.1}\right)^{22/3}$$
$$\sim \left(\frac{D}{2\times10^{20}\ \mathrm{cm}}\right)^3 \left(\frac{x/\bar{x}}{0.4}\right)^{-90/7} \left(\frac{M_{BH}}{0.5M_\odot}\right)^{-2/7} \left(\frac{\Omega h^2}{0.1}\right)^{30/7}. \tag{7.7}$$

Therefore, if $D>2\times10^{20}$ cm, $|\dot{J}^{(GW)}/\dot{J}^{(tidal)}|>1$ for a binary with the semimajor axis $a\lesssim2\times10^{15}$ cm, which corresponds to $x/\bar{x}\lesssim0.4$. If the scale factor R becomes larger than $\sim10^3$, the mean separation becomes larger than 2×10^{20}, and so the tidal force can be neglected. In the matter dominated era R is given by $(t/t_{eq})^{2/3}$, and so $t\sim10^{9/2}t_{eq}$ at $R\sim10^3$, where $t_{eq}=\sqrt{3/8\pi\rho_{eq}}=\sqrt{\bar{3x^3}/8\pi M_{BH}}$ is the equality time. The increase of the angular momentum ΔJ during $t_{eq}<t<10^{9/2}t_{eq}$ by the tidal force can be estimated as

$$|\Delta J| \sim \int_{t_{eq}}^{10^{9/2}t_{eq}} \dot{J}dt \sim \int_{t_{eq}}^{10^{9/2}t_{eq}} \frac{M_{BH}^2a^2}{D^3}dt$$
$$\sim \int_{t_{eq}}^{10^{9/2}t_{eq}} \frac{M_{BH}^2a^2}{\bar{x^3}(t/t_{eq})^2}dt \sim \frac{M_{BH}^2a^2t_{eq}}{\bar{x^3}}. \tag{7.8}$$

The ratio of the increase of the angular momentum during $t_{eq}<t<10^{9/2}t_{eq}$ to the initial angular momentum of the binary at the formation is given by

$$|\Delta J/J| \sim \frac{M_{BH}^2a^2t_{eq}/\bar{x^3}}{b\sqrt{M_{BH}/2a}} = \sqrt{\frac{3\alpha^3}{4\pi\beta^2}} \left(\frac{x}{\bar{x}}\right)^3 \left(\frac{y}{\bar{x}}\right)^3$$
$$= \sqrt{\frac{3\alpha^3}{4\pi\beta^2}} \left(\frac{t}{\bar{t}}\right)^{-1/7} \left(\frac{x}{\bar{x}}\right)^{58/7}$$
$$\sim \left(\frac{x/\bar{x}}{0.5}\right)^{58/7} \left(\frac{M_{BH}}{0.5M_\odot}\right)^{5/21} \left(\frac{\Omega h^2}{0.1}\right)^{16/21}, \tag{7.9}$$

where we used Eqs. (2.4) and (2.5) in the second equality.

We used Eq. (5.6) in the third equality and we set $\alpha=0.4$, $\beta=0.8$ and $t\sim t_0$ in the last equality. Therefore, if $x/\bar{x}<0.4$, which corresponds to most binaries that coalescence at $t\sim t_0$, as can be seen from Fig. 4, the increase of the angular momentum during $t_{eq}<t<10^{9/2}t_{eq}$ can be neglected.

To conclude, the tidal force from the other bodies can be neglected if the binary is separated from the other bodies by greater than the mean separation. More detailed calculations taking N-body effects into account are needed to confirm the above arguments on the effect of the tidal force of the other body on the evolution of the binary parameters after formation. The signs of the change rate of the energy and the angular momentum in Eqs. (7.3) and (7.6) are not certain so that we argued only sufficient conditions. Moreover, if the binding energy of the binary does not change secularly but periodically under the influence of the tidal field, Eq. (7.3) may be an overestimate. So the effect of the tidal field may be weaker.

VIII. SUMMARY

In this paper we have discussed black hole binary formation through three body interactions in the expanding universe. We have confirmed that the order-of-magnitude argument in Ref. [15] is valid within an error of $\sim 50\%$. Several effects have been considered. The effect of the 3-body collision and the mean fluctuation field may reduce the event rate of the coalescing BHMACHO binaries by about one-half. On the contrary the angle dependence of the tidal force may increase the event rate about twice. The results do not crucially depend on the initial peculiar velocity of BHMACHOs and the initial scale factor when the BHMACHOs begin to interact. The radiation drag does not affect the motion of BHMACHOs. After all, the probability distribution function for the coalescence time $f_t(t)$ in Eq. (5.8) is a good estimate. The error in the event rate estimate can be obtained by considering the minimum event rate. The minimum event rate can be estimated as $\{1\times10^{-1}$[original estimate by f_t(t)]$\}$ $\times$[40%(3-body collision effect+mean fluctuation field effect)]$\times$[30%(maximum initial peculiar velocity effect)]$\sim 1.2\times10^{-2}$ events/yr/galaxy. Then the event rate will be $5\times10^{-2}\times2^{\pm1}$ events/yr/galaxy including the uncertainty from the various effects in a plain fashion. This suggests that we can at least expect several events per year within 15 Mpc even when the event rate is minimum, 1×10^{-2} events/yr/galaxy. This event rate of coalescing BHMACHO binaries is comparable to or greater than the upper limit of that of coalescing binary neutron stars [25]. The gravitational wave from such coalescence should be able to be detected by LIGO-VIRGO-TAMA-GEO network.

We have simplified the real situation to the three body problem, so that N-body effects have not been fully taken into account. They are (1) the destruction of the formed binary by the 3-body collision between the binary and the infalling body after the equal time, (2) the deformation of the orbit by the tidal field from the other body, and so on. Although these effects have been estimated in Sec. VII and the event rate estimate does not seem to be influenced by these effects; more detailed calculations taking N-body effects into account are needed to confirm this conclusion. It is possible to investigate the N-body effect by N-body numerical simulations. However, the dynamical range of a is very large (10^5 cm$<a<10^{16}$ cm), and so we need to perform numerical simulations with a large dynamic range using the biggest supercomputer. This is an important, challenging numerical problem.

Throughout this paper, we assumed that all BHMACHOs have the same mass, although we have outlined the extension to the unequal mass case in the Appendix. This is based on the assumption of a delta-function-type density fluctuation at the formation. Even in this case of the delta-function-type density fluctuation, there is a suggestion that in reality the IMF of primordial black holes may continue down to the zero mass limit [32]. However, the IMF in this case has a steep rise proportional to $\sim M^3$ at the lower mass end and an exponential cutoff near the horizon mass. Hence the picture of the delta-function-like IMF seems to be valid. However, in the case of a general spectrum of the density fluctuation, we should consider binaries made from different mass BHMACHOs.

Although we have assumed that the initial distribution of BHMACHOs is random, the high density region may have a strong correlation. Presumably this depends on the black hole formation process or the initial density perturbation spectrum. If a strong correlation existed, more binary BHMACHOs may be formed. This is also an interesting future problem.

ACKNOWLEDGMENTS

We would like to thank Professor H. Sato for continuous encouragement and useful discussions. We are also grateful to N. Sugiyama, K. Nakao, R. Nishi, T. Tsuchiya and D. Ida for useful discussions, and S. A. Hayward for a careful reading of the manuscript. This work was supported by a Grant-in-Aid of the Ministry of Education, Culture, and Sports, No. 09640351.

APPENDIX: EXTENSION TO THE UNEQUAL MASS CASE

In this appendix, we estimate the semimajor axis and semiminor axis of the BHMACHO binary with unequal mass. We only give an order-of-magnitude estimate along the line of Ref. [15] and Sec. II.

We describe the mass function of black holes as $F(M)$, which is normalized as $\int_0^\infty F(M)dM=1$. The average mass of black holes, $\bar{M}_{BH}$, can be obtained as $\bar{M}_{BH}=\int_0^\infty MF(M)dM$. The mean separation of black holes at the time of matter-radiation equality is given by $\bar{x}=(\bar{M}_{BH}/\rho_{eq})^{1/3}$, where we assumed that the average in space is equal to the ensemble average. Consider a pair of black holes with masses M_1 and M_2 and a comoving separation x. This pair will decouple from the cosmic expansion if its mean energy density $\bar{\rho}_{BH}=(M_1+M_2)/(2x^3R^3)$ becomes larger than the radiation energy density $\rho_r=\rho_{eq}/R^4$. In terms of R, this condition can be written as

$$R > R_m \equiv \left(\frac{2\bar{M}_{BH}}{M_1+M_2}\right)\left(\frac{x}{\bar{x}}\right)^3 = \xi\left(\frac{x}{\bar{x}}\right)^3, \tag{A1}$$

where $\xi = 2\bar{M}_{BH}/(M_1+M_2)$. The semimajor axis a will be proportional to xR_m and is given by

$$a = \tilde{\alpha}\left(\frac{2\bar{M}_{BH}}{M_1+M_2}\right)\frac{x^4}{\bar{x}^3} = \xi\tilde{\alpha}\frac{x^4}{\bar{x}^3}, \tag{A2}$$

where $\tilde{\alpha}$ is a constant of order $O(1)$. Consider a black hole with mass M_3 in the nearest neighborhood of the binary. Let its comoving separation from the center of mass of the binary be y. Then the semiminor axis b will be proportional to (tidal force)$\times$(free fall time)^2 and is given by

$$b = \tilde{\alpha}\tilde{\beta}\left(\frac{M_3 x R_m}{(yR_m)^3}\right)\left(\frac{(xR_m)^3}{(M_1+M_2)/2}\right) = \left(\frac{2M_3}{M_1+M_2}\right)\tilde{\beta}\left(\frac{x}{y}\right)^3 a = \eta\tilde{\beta}\left(\frac{x}{y}\right)^3 a, \tag{A3}$$

where $\tilde{\beta}$ is a constant of order $O(1)$ and $\eta = 2M_3/(M_1+M_2)$. $\tilde{\alpha}$ and $\tilde{\beta}$ may depend on mass.

If we assume that black holes are formed randomly, then the probability distribution function $P(x,y,M_1,M_2,M_3)$ is

$$P(x,y,M_1,M_2,M_3)dxdydM_1dM_2dM_3 = \frac{9x^2y^2}{\bar{x}^6}e^{-y^3/\bar{x}^3}dxdyF(M_1)F(M_2)F(M_3)dM_1dM_2dM_3, \tag{A4}$$

where we assumed that x, y do not depend on mass. Equation (5.4) can be written in terms of x and y using Eqs. (A2) and (A3) as

$$t = \tilde{t}\left(\frac{x}{\bar{x}}\right)^{37}\left(\frac{y}{\bar{y}}\right)^{-21}, \tag{A5}$$

$$\tilde{t} = (\eta\tilde{\beta})^7\left(\frac{\xi\tilde{\alpha}\bar{x}}{a_0}\right)^4 t_0. \tag{A6}$$

Integrating Eq. (A4) for a given t with the aid of Eq. (A5), we obtain the probability distribution function of the coalescence time $f_t^{uneq}(t)$ for the unequal mass case. We should take the range of the integration as $0 < x < \xi^{-1/3}\bar{x}$, $x < y < \infty$. The first condition $x < \xi^{-1/3}\bar{x}$ is necessary for binary formation so that $R_m < 1$. The second condition turns out to be $(t/\tilde{t})^{1/16}\bar{x} < y < \xi^{-37/63}(t/\tilde{t})^{-1/21}\bar{x}$ for a given t. Performing the integration, we have

$$f_t^{uneq}(t)dt = \int_0^\infty\int_0^\infty\int_0^\infty \frac{3}{37}\left(\frac{t}{\tilde{t}}\right)^{3/37} \times\left[\Gamma\left(\frac{58}{37},\left(\frac{t}{\tilde{t}}\right)^{3/16}\right)-\Gamma\left(\frac{58}{37},\xi^{-37/21}\left(\frac{t}{\tilde{t}}\right)^{-1/7}\right)\right]\frac{dt}{t} \times F(M_1)F(M_2)F(M_3)dM_1dM_2dM_3. \tag{A7}$$

To integrate the above equation with mass, we need accurate values of $\tilde{\alpha}$ and $\tilde{\beta}$, as well as assuming the form of the mass fuction $F(M)$. This is left as a future problem.

[1] C. Alcock *et al.*, Astrophys. J. **486**, 697 (1997).
[2] M. Pratt, in Proceedings of the 3rd Microlensing Workshop, 1997 (unpublished).
[3] J. N. Bahcall, C. Flynn, A. Gould, and S. Kirhakos, Astrophys. J. Lett. **435**, L51 (1994).
[4] C. Flynn, A. Gould, and J. N. Bahcall, Astrophys. J. Lett. **466**, L55 (1996).
[5] D. S. Graff and K. Freese, Astrophys. J. Lett. **456**, L49 (1996); **467**, L65 (1996).
[6] D. Ryu, K. A. Olive, and J. Silk, Astrophys. J. **353**, 81 (1990).
[7] S. Charlot and J. Silk, Astrophys. J. **445**, 124 (1995).
[8] B. K. Gibson and J. R. Mould, Astrophys. J. **482**, 98 (1997).
[9] R. Canal, J. Isern, and P. Ruiz-Lapuente, Astrophys. J. Lett. **488**, L35 (1997).
[10] G. Chabrier, L. Segretain, and D. Mera, Astrophys. J. Lett. **468**, L21 (1996).
[11] F. C. Adams and G. Laughlin, Astrophys. J. **468**, 586 (1996).
[12] B. D. Fields, G. J. Mathews, and D. N. Schramm, Astrophys. J. **483**, 625 (1997).
[13] T. Nakamura, Y. Kan-ya, and R. Nishi, Astrophys. J. Lett. **473**, L99 (1996).
[14] Y. Fujita, S. Inoue, T. Nakamura, T. Manmoto, and K. E. Nakamura, Astrophys. J. Lett. **495**, L85 (1998).
[15] T. Nakamura, M. Sasaki, T. Tanaka, and K. S. Thorne, Astrophys. J. Lett. **487**, L139 (1997).
[16] J. Yokoyama, Astron. Astrophys. **318**, 673 (1997).
[17] M. Kawasaki, N. Sugiyama, and T. Yanagida, Phys. Rev. D **57**, 6050 (1998).
[18] K. Jedamzik, Phys. Rev. D **55**, 5871 (1997).
[19] P. J. E. Peebles, *The Large-Scale Structure of the Universe* (Princeton University Press, Princeton, 1980).
[20] T. Futamase, Mon. Not. R. Astron. Soc. **237**, 187 (1989); Phys. Rev. D **53**, 681 (1996); T. Futamase and M. Sasaki, *ibid.* **40**, 2502 (1989).
[21] M. Shibata and H. Asada, Prog. Theor. Phys. **94**, 11 (1995).
[22] W. H. Press *et al.*, *Numerical Recipes in Fortran*, 2nd ed. (Cambridge University Press, Cambridge, England, 1992).
[23] D. P. Bennett *et al.*, Nucl. Phys. B (Proc. Suppl.) **51B**, 152 (1996).
[24] P. C. Peters, Phys. Rev. **136**, B1224 (1964).
[25] E. S. Phinney, Astrophys. J. Lett. **380**, L17 (1991).

[26] R. Narayan, T. Piran, and A. Shemi, Astrophys. J. Lett. **379**, L17 (1991).
[27] E. P. J. van den Heuvel and D. R. Lorimer, Mon. Not. R. Astron. Soc. **283**, L37 (1996).
[28] V. Szebehely and K. Zare, Astron. Astrophys. **58**, 145 (1977).
[29] C. Hogan, Mon. Not. R. Astron. Soc. **185**, 889 (1978).
[30] S. Chandrasekhar, Astrophys. J. **97**, 255 (1943).
[31] J. Binney and S. Tremaine, *Galactic Dynamics* (Princeton University Press, Princeton, 1980).
[32] J. C. Niemeyer and K. Jedamzik, Phys. Rev. Lett. **80**, 5481 (1998).